



Strained noble metal di chalcogenides PtX₂ (X = S, Se) mono-layer: Ab initio study of electronic and lattice dynamic properties

Sohail Ahmad

Department of Physics, College of Science, King Khalid University, P. O. Box 9004, Abha, Saudi Arabia

ARTICLE INFO

Keywords:

Strain
Electronic properties
Vibrational spectrum
Monolayer
PtS₂
PtSe₂

ABSTRACT

Electronic properties of noble metal dichalcogenides PtX₂ (X = S, Se) mono-layers have been studied using plane wave pseudopotential method based on density functional theory. The band gap is observed to be as 1.94 eV (1.37 eV) in case of PtS₂ (PtSe₂) mono-layer which is found to be in close agreement with previous known results. A further variation in band gap is observed in both the two mono-layers on applying biaxial tensile as well as compressional strain. Phonon spectrum of these mono-layers and its strained structure reflects its dynamical stability.

1. Introduction

After the successful synthesis of graphene [1–3], a new wave of research has also been taking place in other two-dimensional (2D) materials such as boron nitride, silicene, germanene and layered transition metal di-chalcogenides (TMDCs) [4–15]. TMDCs, especially their two-dimensional (2D) counterparts, are a class of materials with fascinating and technologically useful properties [16,17]. Depending on the stoichiometry, the three-dimensional TMDCs with a formula MX₂, where M represents transition metals and X is chalcogen, can be either metals or semiconductors with indirect band gaps. Whereas the 2D monolayers are direct-band-gap semiconductors with sizable band gaps around 1–2 eV [18]. This band-gap phenomenon together with the versatile chemistry of MX₂ enables a variety of fields of applications including field-effect transistors, energy storage, and catalysis [16–19]. Several TMDCs (e.g., MoS₂, MoSe₂, and WS₂) have been extensively investigated, both experimentally and theoretically [20–27] however there are not many studies of platinum and palladium dichalcogenides.

It has been demonstrated that noble metals, like Pt and Pd can also form layered structures with S atoms [28–31]. Inspired by the extensive studies of 2D TMDCs, it is expected that PdS₂ and PtS₂ can also be exfoliated into a mono-layer and find some important applications in electronics. First principles calculations suggest semiconducting behavior for monolayer PdSe₂ with indirect gap value of 1.43 eV. [32]. Monolayer of PtSe₂ has been grown experimentally [33] by direct selenization on a Pt substrate and the semiconducting behavior with band gap of 1.20 eV was observed in it. There are very few studies on mono-layer chalcogenides of Pt and Pd. Miro et al. [34] theoretically studied the electronic properties of PdS₂ and PtS₂ mono-layer and

found these mono-layers as semiconducting with band gap 1.17 eV and 1.78 eV respectively. However, they reported that the most stable configuration of these mono-layers is 1 T, which is different from that of the layers in PtS₂ bulk. Very recently we carried out ab initio calculations to study the strain dependent electronic properties of PdS₂ and PdSe₂ mono-layers in 1 T phase [35]. To extend our work, here we report results of strain induced tuning electronic properties of mono-layers of sulfides and selenides of Pt. A trend in band gap variation with strain is discussed. Phonon spectrum of PtX₂ (X = S, Se) and its strained structure have also been studied to check the stability of system.

2. Computational methodology

We used the plane wave pseudo potential method as implemented in the QUANTUM-ESPRESSO code [36] to perform all the calculations. The exchange correlation potential was approximated by generalized gradient approximation using Perdew-Burke-Ernzerhof exchange-correlation functional [37]. We used norm conserving ultra-soft pseudopotentials for Pt, S and Se each. The atomic positions and cell parameters were fully relaxed until an energy convergence of 10⁻⁹ eV reached. We used wave function and charge density cutoffs of 70 Ryd and 300 Ryd, respectively. A large vacuum layer of 15 Å was adopted to prevent the interaction between adjacent images. Optimized structure (co-ordinates) was used to perform self-consistent calculations with a Monkhorst-Pack [38] 16 × 16 × 1 k-mesh followed by the non-self-consistent calculations for band structures, density of states and partial density of states of PtX₂ mono-layer. We followed 120 × 120 × 1 k-points mesh along the path Γ -M-K- Γ in the irreducible Brillouin zone to

E-mail address: sohail@kku.edu.sa.

<http://dx.doi.org/10.1016/j.physe.2017.09.016>

Received 17 February 2017; Received in revised form 16 September 2017; Accepted 19 September 2017

Available online 21 September 2017

1386-9477/© 2017 Elsevier B.V. All rights reserved.

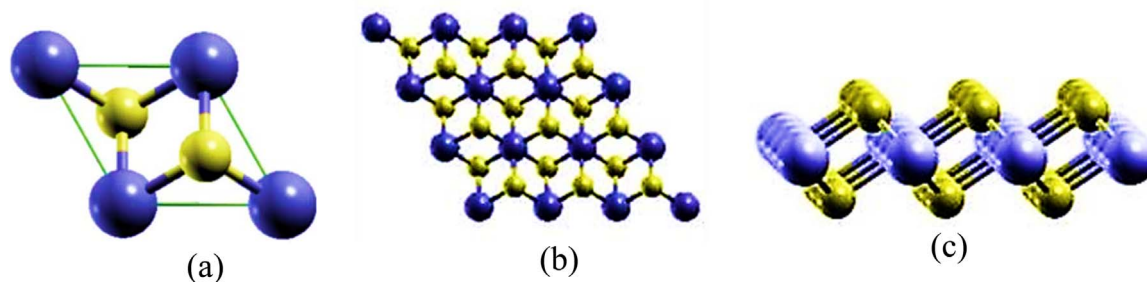


Fig. 1. PtX₂ mono-layer crystal structure (a) unit cell (b) top view (b) side view. Blue color represents Pt while yellow represents chalcogenides X (X = S, Se). (For interpretation of the references to color in this figure legend, the reader is referred to the web version of this article.).

obtain the band structure with a very fine mesh points. A uniform bi-axial tensile and compression strain ranging upto 8% with increment of 2% were applied on mono-layer PtX₂ to study the change in behavior of its electronic properties. To determine the phonon spectrum of PtX₂, we used $16 \times 16 \times 1$ *k*-mesh and $2 \times 2 \times 1$ *q*-mesh respectively.

3. Results and discussion

We studied platinum disulphides and diselenides mono-layers in 1 T polytypic form as shown in the Fig. 1. The unit cell consists of one Pt and two chalcogenides whose coordinates and lattice constants are mentioned in Table 1. The band structure and density of states (DOS) of PtX₂ (X = S, Se) mono-layers have been studied. As shown in Fig. 2, where the Fermi level is set at zero, PtS₂ mono-layer is a semiconductor with indirect band gap of ca. 1.94 eV. The band structure shown in the Fig. 2 may be divided into three main groups. The band structure in the range zero to 3 eV in conduction band region is mainly contributed by Pt(*d*) and X(*p*) orbitals and similarly in the range 0 to –6 eV in valence band region is contributed by Pt(*d*) and X (*p*) orbitals. On the other hand, Pt(*p*) and X(*s*) contribute mainly to the band structure in the range –12 to –15 eV. These findings are in good agreement with previous reported results [19,39]. After getting confirmation about the results for PtS₂, we proceeded further to study PtSe₂ mono-layer and we got a similar behavior except that the energy band gap in this case as 1.37 eV which is in good agreement with the previous results [39,40]. The density of states for PtSe₂ mono-layer are similar to those of PtS₂ with some minor differences. Our band structures for PtS₂ and PtSe₂ show good agreement with the earlier available data in the matter of valence band maxima (VBM) and conduction band minima (CBM) locations [19,39,40]. Our calculated energy gaps are also mentioned in Table 1 along with other previous known results. The difference may be due to different level of accuracy and the calculation methodologies

Table 1
Structural parameters and energy band gap (along with previous known results) for optimized PtX₂ (X = S, Se) mono-layer.

PtX ₂	Co-ordinates (Å)	<i>d</i> _{Pt-X} (Å)	<i>d</i> _{X-X} (Å)	<i>E</i> _g (eV)
PtS ₂	Pt (0.00000000, 0.00000000, 0.00000000)	2.42,	3.26	1.94
	S (1.80374761, 1.02664090, 1.24494353)	2.37 ^a		1.78 ^a
	S (–1.80374761, –1.02664090, –1.24494353)			1.69 ^b
PtSe ₂	Pt (0.00000000, 0.00000000, 0.00000000)	2.53,	3.54	1.37
	Se (1.84415935, 1.03304067, 1.40057089)	2.57 ^a		1.12 ^a
	Se (–1.84415935, –1.03304067, –1.40057089)			1.25 ^b
				1.20 ^c

^a Ref. [19].

^b Ref. [39].

^c Ref. [40].

adopted in the calculations. Experimentally, the controllable band gap engineering of nanomaterials is always desirable for a wide range of applications. It is well established that strain can efficiently modify the electronic properties of many 2D structure. Hence, we investigated the influence of uniform bi-axial tensile as well as compressional strain on the band structure modulation of PtS₂ and PtSe₂ mono-layers. Here the strain (ϵ) is defined as $\epsilon = (l - l_0)/l_0$, where *l* and *l*₀ are the strained and the equilibrium lattice constants of the PtX₂ mono-layers, respectively. Our computations demonstrated that the effect of bi-axial strain is pronounced as shown in the Fig. 3. The irreducible Brillouin Zone of PtX₂ under uniform bi-axial tensile strain remains unchanged. Upon applying a 2% bi-axial tensile strain in both *x* and *y* directions (*xy*), the band gap of PtS₂ decreases to indirect band gap of 1.78 eV while VBM and CBM remain at the same points respectively (not shown in the figure). When the bi-axial tensile strain increases to 4%, the CBM is still located at the same point whereas the VBM is relocated to a point (A) between Γ and M, and the band gap decreases to direct band gap of 1.61 eV as shown in the Fig. 3b. On further increase of strain (till 8%), a linear decrease in band gap up to 1.20 eV is observed. A decrease in band gap up to 1.42 eV is observed on applying bi-axial compression till 8%. The equilibrium lattice constants and band gap along with Lowdin population analysis for each strained structure are mentioned in Table 2. The partial density of states (PDOS) analysis reveals as shown in Fig. 4 that the conduction band minima are contributed mainly by S-3*p* (*p_z* & *p_y*) and Pt-4*d* (*d_{xy}* & *d_{zy}*) by equal weight while the valence band maxima are contributed by S-3*p* (*p_x* & *p_y*) and partially by Pt-4*d* (*d_z²*, *d_{xy}* & *d_{zy}*). In CBM, *p_x* & *p_y* orbital of S-3*p* are degenerate. On applying biaxial tensile strain, the contributions from S(*p_z*) and Pt(*d_z²*) become more prominent. A monotonous decrease in band gap from 1.37 to 0.79 eV (0.52 eV) is observed on applying bi-axial tensile (compression) strain in case of PtSe₂ mono-layer as shown in Fig. 3. Like PtS₂, the unstrained and strained mono-layer PtSe₂ have similar state contributions of different orbitals around the Fermi level as shown in Fig. 4. The variation of band gap with different value of biaxial tensile and compression strain are also shown in Fig. 5. The strain dependent band gap modulation study in these materials is being made for the first time so there is no available data to compare with but a similar variation in band gap has been observed in other transition metal di chalcogenides mono-layers [23,35,41,42]. Based on Lowdin population analysis, it is confirmed that on applying biaxial tensile (compression) strain the charge density around chalcogenides increases (decreases) while it decreases (increases) around transition metals.

To gain further insight into this study, we also calculated the phonon dispersions which are an interesting characteristic of the material. Phonons play a significant role in the study of transport and optical properties and hence their accurate description is extremely important [43]. In the present contribution, the phonon dispersion curves have been computed along high symmetry directions in the Brillouin zone for unstrained and biaxial compressional strained mono-layer of PtS₂ and PtSe₂. Our results for unstrained and strained (–4%) mono-layer PtS₂ and PtSe₂ are shown in Fig. 6. The phonon

Download English Version:

<https://daneshyari.com/en/article/5450064>

Download Persian Version:

<https://daneshyari.com/article/5450064>

[Daneshyari.com](https://daneshyari.com)